

Studies on the Interaction of Alkyl Thiophosphinate with Precious Metals

Dong Su Kim

*Department of Environmental Engineering, Ewha Womans University, Seoul 120-750, Korea

Received November 29, 1994

Adsorption mechanisms of diisobutyl dithiophosphinate (DIBDTPI) and diisobutyl monothiophosphinate (DIBMTPI) on gold and gold-silver alloys (80:20 and 50:50) have been studied. The adsorption mechanisms on gold-silver alloys can be explained by the EC mechanism involving an electron transfer step and a chemical reaction step. Thus, the adsorption should be controlled by the E of the electrochemical oxidation of the electrode involved and the pK of the metal collector complex. Both di- and mono- thiophosphinate adsorb on 50:50 Au-Ag alloy at lower potential than on 80:20 Au-Ag alloy surface. There are no significant differences between the reactivities of DIBDTPI and DIBMTPI with precious metals except that the dithio- compound can be oxidized to dimer on gold at high potentials, while the monothio- homologue cannot. In this regard, DIBDTPI may be a better surface active reagent for pure gold than DIBMTPI.

Introduction

The sulfur analogues of phosphinic acids have recently found wide acceptance as selective collectors for the flotation separation of base metal sulfides and precious metals, specially from complex sulfide ores.^{1,2} The dithiophosphinate (DTPI) is structurally similar to dithiophosphate (DTP, see Table 1) but has collector properties that are quite different from that of DTP. The metal complexes of DTPI are several orders of magnitude more stable than those of DTP.¹ The DTPI is also more resistant to aqueous oxidation than DTP. The dialkyl DTPI is a far superior collector for galena, chalcopyrite and precious metal values, as well as more selective against sphalerite and iron sulfides, than the corresponding DTP.

The monothiophosphinate (MTPI) is a new collector derived from the corresponding dithiophosphinate by replacing one of the sulfur atoms with oxygen (Table 1). This change results in a more stable and stronger collector under certain pH conditions.³⁻⁵ As in the case of the dithio analogues, there are differences in collector properties between MTPI and monothiophosphate (MTP). The MTPI, being a weaker acid than MTP, is more effective in the neutral and mildly alkaline pH conditions. The use of MTPI has also been shown to provide increased precious metals recoveries from ores.

It is well established that the adsorption of xanthate occurs *via* a mixed potential mechanism, involving the anodic oxidation of xanthate and the cathodic reduction of oxygen.⁶ The adsorption of xanthate results either in the formation of di-xanthogen or metal xanthate. In the first case, the mineral itself does not participate in the reaction except offering a passage for the transfer of electron. This would be the case for xanthate adsorption on pyrite, pyrrhotite, and gold.

For the case of xanthate adsorbing on some of the other sulfide minerals (*e.g.*, chalcocite and galena), the mineral itself is participating in the adsorption process resulting in the formation of metal xanthates. The mechanism may be viewed as a two-step process involving an initial electrochemical reaction (E), which is the oxidation of the mineral

Table 1. Structure of thiophosphate and thiophosphinate collectors

Dithiophosphate (DTP)	Dithiophosphinate (DTPI)
$\begin{array}{c} \text{S} \\ \parallel \\ \text{R-O} \text{---} \text{P} \text{---} \text{S}^- \\ \diagup \quad \diagdown \\ \text{R-O} \end{array}$	$\begin{array}{c} \text{S} \\ \parallel \\ \text{R} \text{---} \text{P} \text{---} \text{S}^- \\ \diagup \quad \diagdown \\ \text{R} \end{array}$
Monothiophosphate (MTP)	Monothiophosphinate (MTPI)
$\begin{array}{c} \text{S} \\ \parallel \\ \text{R-O} \text{---} \text{P} \text{---} \text{O}^- \\ \diagup \quad \diagdown \\ \text{R-O} \end{array}$	$\begin{array}{c} \text{S} \\ \parallel \\ \text{R} \text{---} \text{P} \text{---} \text{O}^- \\ \diagup \quad \diagdown \\ \text{R} \end{array}$

to release the metal ions, followed by the chemical reaction (C) between the metal ions and xanthate to form metal xanthate. In organic electrochemistry, such mechanisms are referred to as coupled electrochemical and chemical reactions of the EC-type.^{7,8}

In the EC mechanism, the electrochemical reaction is controlled by the electrochemical potential (E) of the system, while the chemical step is controlled by its stability constant (pK), as suggested by the chemical theory of collector adsorption.⁹ It may be stated, therefore, that the adsorption of thiol collectors on sulfides is controlled by both the E and pK values of the system. The E determines the availability of metal ions, while the pK of the metal thiol complex determines whether this complex can be formed. The EC mechanism simplifies the understanding of the adsorption process, specifically for cases where the mineral itself undergoes oxidation and participate in the adsorption reactions.

The EC mechanism was employed to explain the adsorption of modified thiol-type collectors, including MTP, on precious metals¹⁰ and that of DTPI on copper and copper sulfides.¹¹ According to the EC mechanism, the process of copper-DTPI formation on copper may be viewed as a two-step process, involving an initial electrochemical reaction (E):



followed by a chemical reaction (C),



The overall reaction then becomes:



However, relatively little is known about the mechanism of interaction of thiophosphinates with precious metals. It is not known whether the precious metals recovery observed in practice is the result of direct interaction with these metals or the result of flotation of sulfides that have physically locked metal values. The validity of the EC mechanism for the precious metal-thiophosphinate system is investigated in the present study using electrochemical and spectroscopic methods.

Experimental

Materials. The gold plate was obtained from Johnson Matthey, while the gold-silver (Au-Ag) alloy plates (0.5 mm thick, 99.9985% pure) were acquired from Kultakeskus Oy (Gold Center), Finland. The same precious metal plates were used in both cyclic voltammetry and FTIR measurements. The ammonium diisobutyl dithiophosphinate (DIBDTPI) and ammonium diisobutyl monothiophosphinate (DIBMTPI) were provided by American Cyanamid Company. The silver diisobutyl dithiophosphinate (AgDIBDTPI) complex was precipitated by mixing silver nitrate and DIBDTPI solutions at neutral pH conditions. Elemental analysis of the precipitate verified it to be AgDIBDTPI. A similar procedure was used in making the silver diisobutyl monothiophosphinate (AgDIBMTPI) complex. The dimer of DIBDTPI was prepared through oxidation with aqueous iodine-potassium iodide solution. The experiments were conducted in 0.05 M $\text{Na}_2\text{B}_4\text{O}_7$ solution (pH 9.2). All reagents used were of analytical grade, and all the solutions were prepared with 18 M Ω water. Prior to each series of electrochemical experiments, the solution was deoxygenated by purging with low-oxygen N_2 gas (<0.05 ppm O_2) for at least one hour.

Cyclic Voltammetry. The cyclic voltammetry experiments were conducted using a conventional three-electrode system with a working electrode holder designed specially for the precious metal plates. The electrode potential was controlled in the electrochemical and spectroscopic measurements with a Pine Instrument Co. Model RDE4 Potentiostat/Galvanostat and a PAR Model 175 Universal Programmer. The reference electrode was a Ag/AgCl electrode, purchased from Fisher Company, in 4 M potassium chloride. All potentials are reported on the standard hydrogen electrode (SHE) scale, taking the potential of the Ag/AgCl electrode to be 0.2 V against the SHE.¹² A scan rate of 50 mV/sec was used in all the cyclic voltammetry experiments and cyclic voltammograms were recorded on a Hewlett Packard 7015B X-Y recorder.

FTIR Spectroscopy. The spectra of the electrode surfaces conditioned at the desired potentials for 1 minute were recorded on a Perkin Elmer 1710 FTIR spectrometer equipped with a mercury cadmium telluride (MCT) detector using

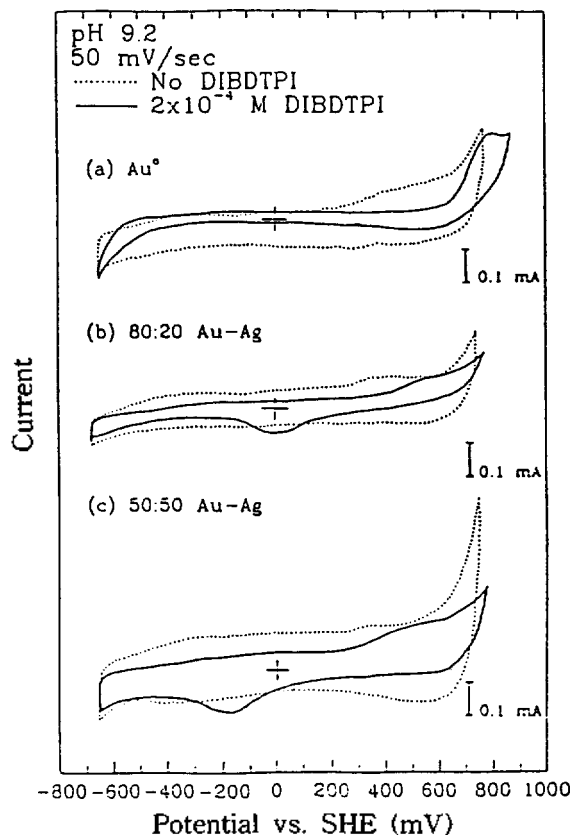


Figure 1. Cyclic voltammograms of (a) Au^0 , (b) 80:20 Au-Ag, and (c) 50:50 Au-Ag at pH 9.2 in 0 (---) and 2×10^{-4} M (—) DIBDTPI.

an external reflection attachment (Spectra Tech) with one reflection. The conditioning potentials were determined according to a result of cyclic voltammetry. The MCT detector was cooled with liquid nitrogen and the angle of incidence was 80° . The spectrometer was purged with N_2 gas to minimize the amount of CO_2 and water vapor present. For each measurement, 100 spectra were scanned, co-added and signal averaged. The spectral resolution was set at 4 cm^{-1} . A wire grid polarizer (Harrick Scientific Corporation) was used to polarize the incident beam parallel to the plane of reflection (*p*-polarized). To obtain the reference spectra, the transmission spectra of DIBDTPI and DIBMTPI in KBr pellets were prepared and measured in the standard way.

Results and Discussion

Diisobutyl Dithiophosphinate. Figure 1 shows the cyclic voltammograms for (a) Au^0 , (b) 80:20 Au-Ag, and (c) 50:50 Au-Ag at pH 9.2 in the absence and presence of 2×10^{-4} M DIBDTPI. In the case of Au^0 , the anodic current starting to rise at above 700 mV in the absence of DIBDTPI is presumably associated with the oxidation of Au^0 . The addition of DIBDTPI results in the passivation of the electrode surface, as indicated by the decrease in the current above 100 mV. However, the IR spectroscopic measurements carried out under similar conditions do not indicate DIBDTPI adsorption in the region where the electrode is passivated. The passivation of the electrode observed in this cyclic volt-

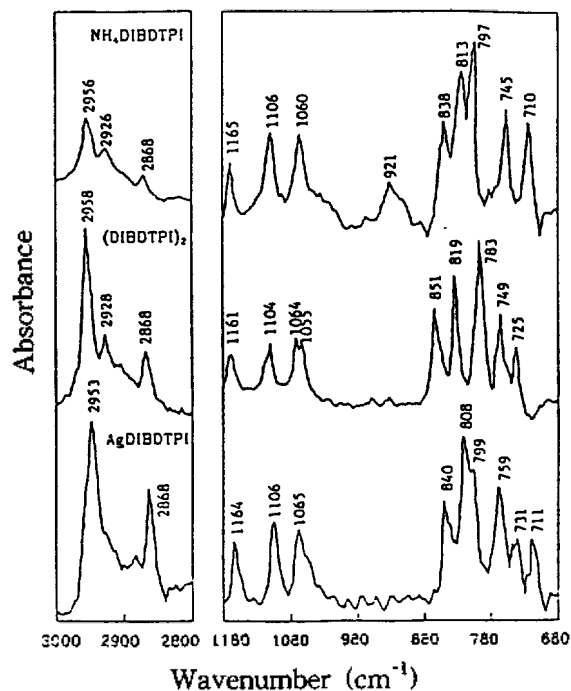


Figure 2. FTIR spectra of $\text{NH}_4\text{DIBDTPI}$, $(\text{DIBDTPI})_2$, and AgDIBDTPI .

ammogram, therefore, may be associated with the weak physisorption of DIBDTPI, which is probably removed from the surface when the sample is rinsed prior to the *ex situ* IR measurements.

At potentials around 600 mV, the anodic current starts to rise. This may be attributed to the oxidation of DIBDTPI according to the following reaction:



Apparently, this reaction is not reversible as there is no well-defined reduction peak shown on the reverse scan. The formation of $(\text{DIBDTPI})_2$ is verified by comparing the FTIR spectrum of surface species with standard spectrum shown in Figure 2.

The cyclic voltammograms for an 80:20 Au-Ag alloy in the absence and presence of 2×10^{-4} M DIBDTPI are shown in Figure 1(b). Without any addition of DIBDTPI, oxygen adsorption on this alloy is indicated by the increase in current above 600 mV. Since the alloy contains 80% of Au^0 by weight, it shows a characteristics quite similar to pure Au^0 . In the presence of DIBDTPI, Ag^0 is passivated below 350 mV. This is probably due to the following reaction:



The proposed DIBDTPI adsorption reaction could be the result of coupled reactions of the EC-type, which has also been suggested for monothiophosphate interaction with Ag^0 .¹⁰ The electrochemical reaction (E) involves the oxidation of Ag^0 :



followed by the chemical step (C):

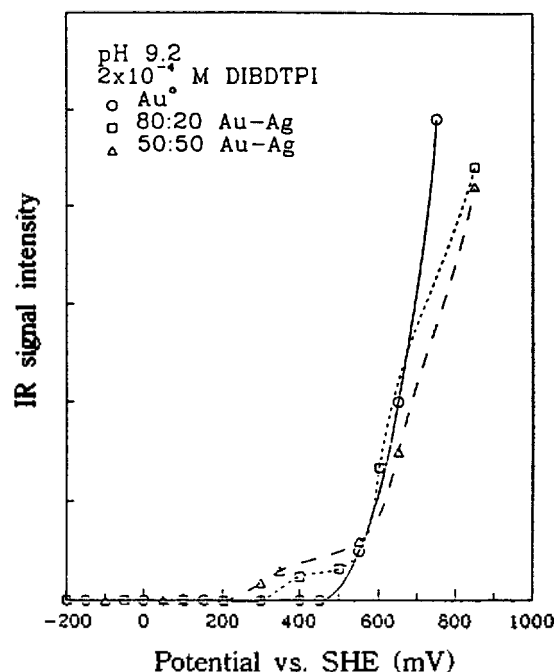


Figure 3. Effect of potential on the IR signal intensity of DIBDTPI adsorbed at 2960 cm^{-1} on Au^0 , 80:20 Au-Ag, and 50:50 Au-Ag.

The interaction of DIBDTPI with the alloy, *via* the EC mechanism, is indicated by the anodic current rise above 350 mV. The oxidation of DIBDTPI to $(\text{DIBDTPI})_2$ is shown by the current rising above 600 mV. The anodic current at higher potentials is due to the oxidation of Ag^0 .

Figure 1(c) shows the results of the cyclic voltmetry obtained for the 50:50 Au-Ag alloy-DIBDTPI system. The voltammograms show that the addition of 2×10^{-4} M DIBDTPI results in the passivation of the electrode at low potentials. The interaction of DIBDTPI on Ag^0 is indicated by the anodic current rising above 300 mV. This value is lower than that for the 80:20 Au-Ag alloy. Therefore, the onset of DIBDTPI adsorption is dependent on the silver content of the alloy. The anodic peak observed at this potential may be attributed to an EC-type reaction mechanism given by reactions (6) and (7). The cathodic current rise starting at around -50 mV is associated with the reverse of reaction (7).

The FTIR spectra obtained for $\text{NH}_4\text{DIBDTPI}$, $(\text{DIBDTPI})_2$, and AgDIBDTPI are given in Figure 2. The major absorption peaks which are characteristic for the $\text{NH}_4\text{DIBDTPI}$ are observed at 2956, 2868, 1165, 1106, 1060, 921, 838, 813, 797, 745, and 710 cm^{-1} . The bands that are characteristic for $(\text{DIBDTPI})_2$ are found at 2958, 2928, 2868, 1161, 1104, 1064, 1055, 851, 819, 783, 749, and 725 cm^{-1} . For the AgDIBDTPI compound, the characteristic bands are observed at 2953, 2868, 1164, 1106, 1065, 840, 808, 799, 759, 731, and 711 cm^{-1} . The bands observed between $3000\text{--}2800 \text{ cm}^{-1}$, which may be associated with the C-H vibrations of the alkyl group,¹³ are almost same for the three DIBDTPI. However, the absorption peaks found below 900 cm^{-1} are shifted for $(\text{DIBDTPI})_2$ and AgDIBDTPI as compared with those for $\text{NH}_4\text{DIBDTPI}$. The signals that may be due to stretching vibration

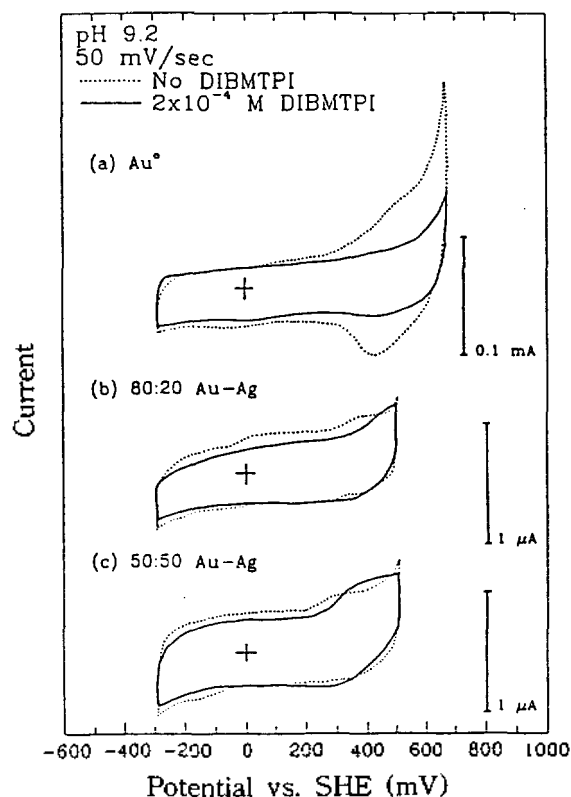


Figure 4. Cyclic voltammograms of (a) Au, (b) 80 : 20 Au-Ag, and (c) 50 : 50 Au-Ag at pH 9.2 in 0 (---) and 2×10^{-4} M (—) DIBMTPI.

of P-S bond^{13,14} are shifted in both cases. This suggests that the sulfur is involved in the bonding, *i.e.*, a S-S bond for (DIBDTPI)₂ and S-Ag bond for AgDIBDTPI.

Figure 3 shows the change in the IR signal intensities measured at 2960 cm^{-1} as a function of applied potentials for Au, 80 : 20 Au-Ag, and 50 : 50 Au-Ag in the presence of 2×10^{-4} M DIBDTPI. It can be seen that DIBDTPI adsorption becomes significant at around 550 mV, 400 mV, and 300 mV for Au, 80 : 20 Au-Ag, and 50 : 50 Au-Ag, respectively. These initial adsorption potentials correspond with those where anodic current rises are observed on the cyclic voltammograms. Therefore, there is a good agreement between the results of electrochemical and spectroscopic measurements. The potential where the collector adsorption starts is directly related to the silver content in the alloys. DIBDTPI adsorption starts at a higher potential for the 80 : 20 Au-Ag alloy than for the 50 : 50 Au-Ag alloy. The reason for this potential shift is considered to be due to the diminished activity of silver as the silver content decreases in the alloy.

Diisobutyl Monothiophosphinate. The cyclic voltammograms for (a) Au, (b) 80 : 20 Au-Ag, and (c) 50 : 50 Au-Ag at pH 9.2 in the absence and presence of 2×10^{-4} M DIBMTPI are presented in Figure 4. The cyclic voltammograms for Au show similar findings to those for the Au-DIBDTPI system, that is, passivation of the electrode is observed. However, there are no indications of the oxidation of DIBMTPI, which is opposite to that observed for the corresponding dithio analogue. The FTIR spectroscopic measure-

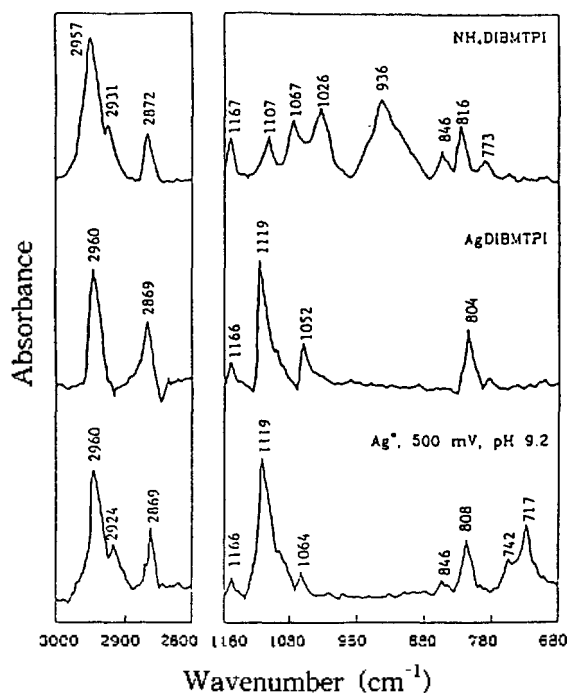


Figure 5. FTIR spectra of NH₄DIBMTPI, AgDIBMTPI, and Ag⁺ conditioned in 2×10^{-4} M DIBMTPI at pH 9.2 and 500 mV.

ments do not indicate the presence of adsorbed species on the Au surface over the entire potential range measured (Figure 6). The passivation observed in this cyclic voltammogram may be attributed to the weak physisorption of DIBMTPI, which the *ex situ* IR reflectance measurement is unable to detect. Similar observations were also made for the Au-MTP systems.¹⁰ The cyclic voltammograms for the 80 : 20 and 50 : 50 Au-Ag alloys are similar to those found for DIBDTPI except that the formation of (DIBMTPI)₂ is not observed for this collector. The adsorption of DIBMTPI on Au-Ag alloys may be attributed to an EC mechanism involving Ag⁺ and DIBMTPI to form AgDIBMTPI. The adsorption mechanism suggested here is similar to that proposed above for the Au-Ag alloy-DIBDTPI system.

Figure 5 shows the FTIR spectra of NH₄DIBMTPI and AgDIBMTPI, and the spectrum obtained for Ag⁺ conditioned at 500 mV. The major absorption bands that are characteristic for the pure reagent are observed at 2957, 2872, 1167, 1107, 1067, 1026, 936, 846, 816, and 773 cm^{-1} . For the AgDIBMTPI, the characteristic bands are observed at 2960, 2869, 1166, 1119, 1052, and 804 cm^{-1} . The bands observed in the 3000-2800 cm^{-1} range, which may be due to the C-H vibration of the alkyl group, do not represent any shift for these two species. On the contrary, the absorption bands observed below 900 cm^{-1} , which is presumably attributed to the stretching vibration of P-S bond, are shifted for AgDIBMTPI. This implies that sulfur is involved in the bonding between silver and DIBMTPI to form AgDIBMTPI. The spectrum obtained for Ag⁺ conditioned at 500 mV in the presence of 2×10^{-4} M DIBMTPI shows characteristic bands which are similar to that for the bulk AgDIBMTPI compound. Therefore, the surface species present on the electrode is thought to be AgDIBMTPI.

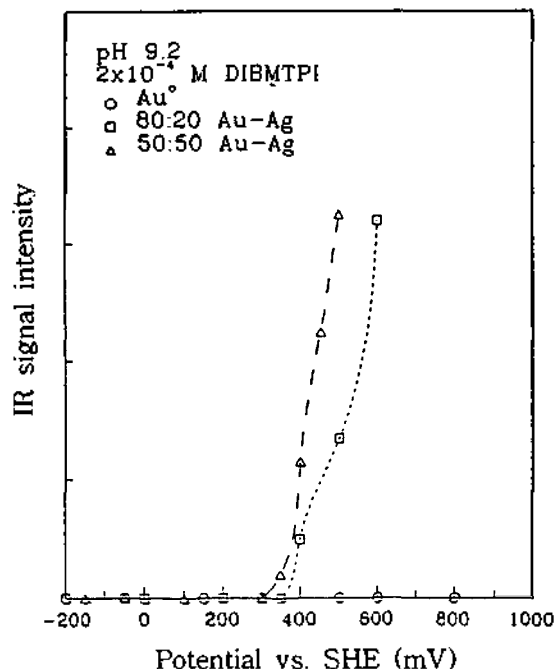


Figure 6. Effect of potential on the IR signal intensity of DIBMTPI adsorbed at 2960 cm^{-1} on Au^0 , 80 : 20 Au-Ag, and 50 : 50 Au-Ag.

Figure 6 shows the change in the IR signal intensities measured at 2960 cm^{-1} as a function of applied potentials for Au^0 and Au-Ag alloys (80 : 20 and 50 : 50) in the presence of $2 \times 10^{-4}\text{ M}$ DIBMTPI. DIBMTPI adsorption becomes significant at around 400 mV and 350 mV for 80 : 20 and 50 : 50 Au-Ag, respectively. However, there is no indication of the presence of adsorbed DIBMTPI on Au^0 over the entire potential range. This result corresponds with that of cyclic voltammetry for Au^0 , which also shows no indications of the oxidation of DIBMTPI. The initial adsorption potentials for Au-Ag alloys correspond with those where anodic current rises are observed on the cyclic voltammograms. Therefore, there is a good agreement between the results of spectroscopic and electrochemical measurements. Same as the case of DIBDTPI, the adsorption starting potential of DIBMTPI on Au-Ag alloys is directly related to the silver content in the alloys. Thus, it may be said that the presence of silver as an alloying element with gold will facilitate the flotation of gold-bearing ores with DIBMTPI.

Summary and Conclusion

The adsorption of diisobutyl di- and mono-thiophosphinates on gold and gold-silver alloys (80 : 20 and 50 : 50) have been studied. The results from cyclic voltammetry and FTIR spectroscopy indicate that the di- and mono-thiophosphinates

adsorb on Au-Ag alloys through the formation of corresponding silver complex via an EC mechanism. The adsorption process involves an initial electrochemical reaction (E), which is the oxidation of silver, followed by the chemical reaction (C) leading to the formation of the Ag-thiophosphinate compound. The results also show that, in the case of diisobutyl dithiophosphinate, both a dimer, $(\text{DIBDTPI})_2$, and silver complexes, AgDIBDTPI , are formed on Au-Ag alloys. On Au^0 electrode, the $(\text{DIBDTPI})_2$ is the only hydrophobic species formed. For the case of DIBMTPI, however, there are no indications of dimer formation on Au^0 and Au-Ag alloys. The potentials for the onset of thiophosphinate adsorption as determined by cyclic voltammetry and FTIR measurements are in good agreement with each other. It is found that the onset potential decreases with increasing silver content of a Au-Ag alloy. The results suggest that the increased precious metals recovery observed in practice when using thiophosphinates is related to their preferred interaction with silver.

References

1. Wang, S. S.; Avotins, P. V. *SME-AIME Annual Meeting*; Dallas, Texas, 1982, Preprint 82-155.
2. Mingione, P. A. *SME-AIME Annual Meeting*; Denver, Colorado, 1991, Preprint 91-33.
3. Nagaraj, D. R.; Avotins, P. V. In *Proceedings of the II International Mineral Processing Symposium*, Aytakin, Y. A. Ed.; Izmir, Turkey, 1988.
4. Nagaraj, D. R.; Lewellyn, M. E.; Wang, S. S.; Mingione, P. A.; Scanlon, M. J. In *Proceedings of the XVI International Minerals Processing Congress*; Forssberg, E. Ed.; Stockholm, Sweden, 1988.
5. Nagaraj, D. R.; Basilio, C. I.; Yoon, R. H. *SME-AIME Annual Meeting*; Las Vegas, Nevada, 1989, Preprint 89-175.
6. Richardson, P. E.; Maust Jr., E. E. In *Flotation*; Fuerstenau, M. C. Ed.; New York, New York, 1976.
7. Nicholson, R. S.; Shain, I. *Anal. Chem.* **1964**, *36*, 706.
8. Southampton Electrochemistry Group. *Instrumental Methods in Electrochemistry*; Halsted Press: New York, U. S. A., 1985.
9. Taggart, A. F.; del Guidice, G. R. M.; Ziehl, O. A. *Trans. SIME*, **1934**, *112*, 348.
10. Basilio, C. I.; Kim, D. S.; Yoon, R. H.; Nagaraj, D. R. *Minerals Engineering* **1992**, *5*, 397.
11. Basilio, C. I.; Yoon, R. H.; Nagaraj, D. R.; Lee, J. *SME-AIME Annual Meeting*; Denver, Colorado, 1991, Preprint 91-171.
12. Bates, R. G. *Determination of pH-Theory and Practice*; John Wiley: New York, U. S. A., 1964.
13. Bellamy, L. J. *The Infrared Spectra of Complex Molecules*; Chapman and Hall: New York, U. S. A., 1975; Vol. 1.
14. Kabachnik, M. I.; Mastryukova, T. A.; Matrosov, E. I.; Fisher, B. *Zhurnal Strukturnof Khimii* **1965**, *6*, 691.
15. Bellamy, L. J. *Advances in Infrared Group Frequencies*; Methuen: London, U. K., 1968.